ACS APPLIED MATERIALS & INTERFACES

Research Article

www.acsami.org

Ultrathin Porous $NiCo_2O_4$ Nanosheet Arrays on Flexible Carbon Fabric for High-Performance Supercapacitors

Jun Du,[†] Gang Zhou,[†] Haiming Zhang,[†] Chao Cheng,[†] Jianmin Ma,[†] Weifeng Wei,[‡] Libao Chen,*[,†] and Taihong Wang[†]

[†]Key Laboratory for Micro-Nano Optoelectronic Devices of Ministry of Education and State Key Laboratory for Chemo/Biosensing and Chemometrics, Hunan University, Changsha 410082, China

[‡]State Key Laboratory for Powder Metallurgy, Central South University, Changsha 410083, China

ABSTRACT: $NiCo_2O_4$ with higher specific capacitance is an excellent pseudocapacitive material. However, the bulk $NiCo_2O_4$ material prevents the achievement of high energy desity and great rate performance due to the limited electroactive surface area. In this work, $NiCo_2O_4$ nanosheet arrays were deposited on flexible carbon fabric (CF) as a high-performance electrode for supercapacitors. The $NiCo_2O_4$ arrays were constructed by interconnected ultrathin nanosheets (10 nm) with many interparticle pores. The porous feature of $NiCo_2O_4$ nanosheets increases the amount of electroactive sites and facilitates the electrolyte penetration. Hence, the $NiCo_2O_4$/CF composites exhibited a high specific capacitance of 2658 F g^{-1} (2 A g^{-1}), good rate performance, and superior cycling life, suggesting the $NiCo_2O_4$/CF is a promising electrode material for flexible electrochemical capacitors.

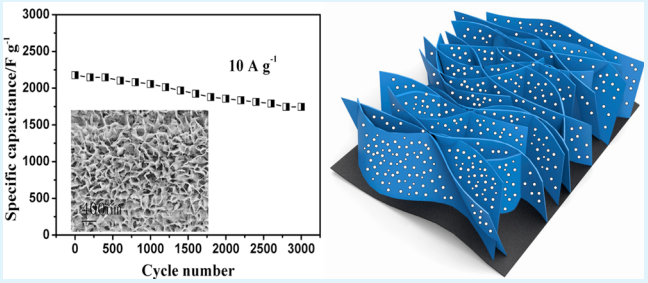

KEYWORDS: *$NiCo_2O_4$, nanosheet arrays, carbon fabric, flexible, supercapacitor*

1. INTRODUCTION

To solve global energy problems, it is high time that researchers developed sustainable and reproducible energy systems. Among them, supercapacitors have attracted increasing interest for great energy devices owing to the excellent characteristics, including fast charge/discharge, high power performance, and great cycling stability.[1] Generally, pseudocapacitors included conductive polymers and metal oxides have higher energy density than the double-layer capacitors.[2−5] RuO_2 is one of typical pseudocapacitive materials because of its high pseudocapacitance (~700 F g^{-1}), excellent reversibility, and high reliability.[6,7] However, Ru is very expensive and rare; the commercial application of RuO_2 as active material in pseudocapacitors has been restricted. Therefore, low-cost transition metal oxides (TMOs), such as MnO_2,[8−10] Fe_2O_3,[11] NiO,[12] and Co_3O_4[13] have been developed as candidates. In particular, the spinel nickel cobaltite ($NiCo_2O_4$) supercapacitors have shown its ultrahigh specific capacitance and rate capabilities, which combined the characteristics of simple TMOs.[14−17] The excellent performances can be attributed to its offering great redox reactions of the cobalt and nickel ions.[18−21]

Recently, some conductive substrates have been used as current collector to improve electrochemical properties of the electrode materials, such as single-walled carbon nanotube[22] and silver naniwire films,[23] which contain the lightweight and flexible characteristics. Carbon fabric (CF) is an ideal conductive substrate for directly growing active material due to the superior electrical conductivity, good flexibility, high mechanical strength and low cost, which can fabricate different types flexible supercapacitors or lithium ion batteries.[24,25] Generally, the coated electrode is used for electrochemical measurement, which contains binder, conductivity agent, and active material. In the electrode, a part of the electroactive sites of active material cannot contact with the electrolyte. Thus, the binder will reduce electrolyte penetration of the active materials and prevent the fast electron transport for high rate capability.[26−28] Therefore, it is necessary to design rational electrode architecture for supercapacitors.[29,30] The ideal electrode for supercapacitors should possess the characteristics of better electrical conductivity for charge transfer and larger specific surface area for ion transport. In this work, we propose a simple strategy to directly grow ultrathin porous $NiCo_2O_4$ nanosheet arrays on flexible CF with excellent electric conductivity and larger specific surface. The $NiCo_2O_4$/CF composites exhibit high specific capacitance of 2658 F g^{-1} (2 A g^{-1}), great rate performance and superior cycling stability in a 3 mol dm^{-3} KOH aqueous electrolyte for high-performance supercapacitors.

2. EXPERIMENTAL DETAIL

2.1. Synthesis. All reagents were of analytical grade and used as without any purification. Before the synthesis, a piece of carbon fabric (CF; ca. 1 cm × 1 cm) was boiled at 100 °C for 1 h with HNO_3 in Teflon-lined autoclave and subsequently rinsed with deionized water

Received: May 8, 2013
Accepted: July 1, 2013
Published: July 1, 2013

   dx.doi.org/10.1021/am4017335 | ACS Appl. Mater. Interfaces 2013, 5, 7405−7409

and absolute ethanol for 15 min. The reaction solution was obtained by mixing 5 mmol of $Ni(NO_3)_2{\cdot}6H_2O$ and 10 mmol of $Co(NO_3)_2{\cdot}6H_2O$ in 20 mL of distilled water under stirring. The $NiCo_2O_4$ precursor was electrodeposited on carbon fabric in the reaction solution at room temperature by using an electrochemical workstation (Chenhua, China). The washed CF was directly used as the working electrode, Hg/Hg_2Cl_2 as reference electrode, and a Pt foil as counter electrode. The electrodeposition potential is −1.0 V (vs SCE). After electrodeposition for 20 min, the sample was rinsed several times by ultrasonication in ethanol amd distilled water and then dried in air. Then, the CF with the as-grown precursors was calcined at 300 °C for 2 h in Ar atmosphere to get the ultrathin porous $NiCo_2O_4$ nanosheet arrays. In average, 0.6 mg of $NiCo_2O_4$ nanosheet arrays is grown per 1 cm × 1 cm of CF carefully weighted after calcination.

2.2. Materials Characterization. The morphologies and microstructures were characterized by scanning electron microscopy (SEM, Hitachi S4800) and transmission electron microscopy (TEM, JEOL 2010). The crystal structure of the materials was determined by X-ray diffraction (XRD, JEOD/ruax2550PC).

2.3. Electrochemical Measurements. The electrochemical measurements were carried out in a three electrode electrochemical cell on a CHI660B electrochemical workstation (Chenhua, China) containing 3 M KOH aqueous solution as the electrolyte. Electrochemical impedance spectroscopy (EIS) was performed with a perturbation potential of 5 mV in a frequency from 100 kHz to 0.1 Hz. A Pt foil was used as the counter electrode and Hg/Hg_2Cl_2 as the reference electrode. The working electrode was an ultrathin nanosheet arrays $NiCo_2O_4$ on CF. The specific capacitance (C) was calculated by the following equations:

$$C = \frac{\int id\Delta u}{v\Delta um} \quad (1)$$

$$C = \frac{it}{\Delta um} \quad (2)$$

where i is discharging current (A), t is discharge time (s), Δu is discharge voltage range (V), v is scan rate (mV s^{-1}), and m is the mass (g) of $NiCo_2O_4$ active materials.

3. RESULTS AND DISCUSSION

The metal hydroxide precursor was prepared by reacting both (Ni^{2+}, Co^{2+}) ions and OH^- which were got by reducing NO_3^- in cathodic. The OH^- ions raised the local pH value of the cathode, resulting in the uniform precipitation of mixed (Ni, Co) hydroxide on the CF surface considering that the solubility product constant (K_{sp}) at 25 °C of $Co(OH)_2$ (2.5×10^{-16}) is very close to $Ni(OH)_2$.[14] Then, the hydroxides were calcined to get $NiCo_2O_4$/CF composites.[29]

The crystal structure of the $NiCo_2O_4$/CF composites were examined by XRD. As Figure 1 reveals, the diffraction peaks at 31.27, 36.26, 44.19, 59.35, 65.23, and 76.70° can be indexed as the (220), (311), (400), (511), (440), and (622) crystal planes of $NiCo_2O_4$ (JCPDS No. 73-1702), respectively. The broad diffraction peaks indicate the poor crystallinity of $NiCo_2O_4$ nanosheet arrays. The diffraction peak at about 24° corresponds to the carbon fabric substrate.

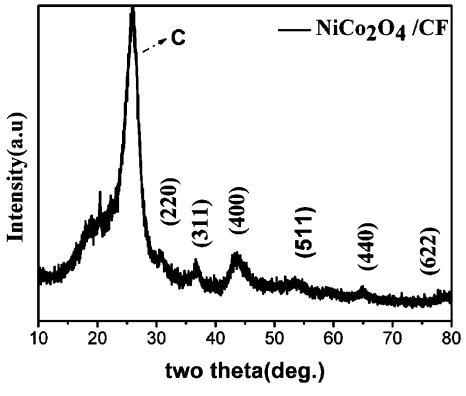

Figure 1. XRD pattern of $NiCo_2O_4$/CF composite.

Figure 2 shows SEM images of the hydroxide precursor and $NiCo_2O_4$/CF nanocomposites. The SEM images in Figure 2a

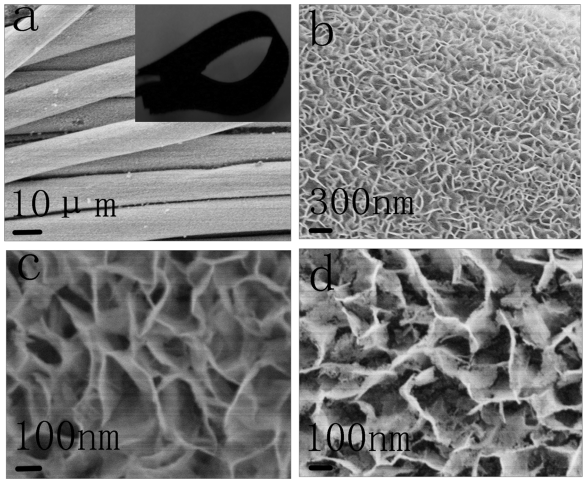

Figure 2. (a−c) SEM images of $NiCo_2O_4$ precursor supported on CF. The inset in part a is an optical image of the precursor supported on CF. (d) FESEM image of the $NiCo_2O_4$/CF composites.

and b show that the hydroxide precursor are uniformly grown on carbon fabric. The $NiCo_2O_4$/CF nanocomposites electrode can keep the original structure after bending and represent great flexibility (the inset Figure 2a). As shown in Figure 2c, the (Ni, Co) hydroxide precursor nanosheets are interconnected with each other and form ordered nanosheet arrays. Moreover, these (Ni, Co) hydroxide precursor nanosheets have a thickness of ca. 10 nm. After heat treatment, the nanosheet arrays are maintained completely, as shown in Figure 2d.

The microstructures and morphologies of the $NiCo_2O_4$/CF nanocomposites were further confirmed by TEM and HRTEM (Figure 3a, b). As Figure 3a shows, the TEM images exhibit

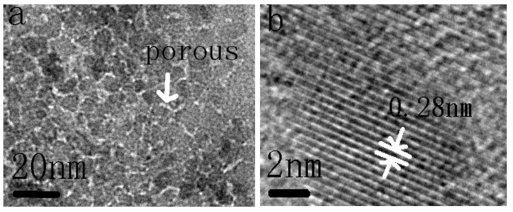

Figure 3. (a) TEM image of the $NiCo_2O_4$/CF composites. (b) HRTEM image of $NiCo_2O_4$nanosheet arrays supported on CF.

that the $NiCo_2O_4$ nanosheets are constructed by multiple $NiCo_2O_4$ particles (diameter ca. 5 nm) and there are a large number of interparticle pores. The porous structure of $NiCo_2O_4$ arrays increases the amount of electroactive sites. The HRTEM image shown in Figure 3b obviously reveals lattice fringes of ca. 0.28 nm, corresponding to the (220) planes of the spinel $NiCo_2O_4$.

Figure 4a displays the electrode architecture of ultrathin porous $NiCo_2O_4$ nanosheet arrays on flexible CF. The binder-

dx.doi.org/10.1021/am4017335 | ACS Appl. Mater. Interfaces 2013, 5, 7405−7409

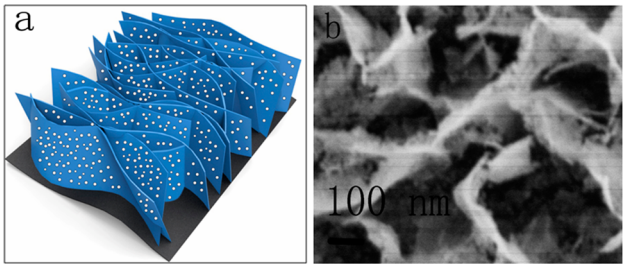

Figure 4. (a) Schematic illustration of ultrathin porous $NiCo_2O_4$ nanosheet arrays on flexible CF. (b) SEM image of the $NiCo_2O_4$/CF composites after 3000 cycles.

free electrode architecture has the following important merits for high-performance supercapacitors. First, the $NiCo_2O_4$ materials directly attached on CF can enhance the electrical conductivity of the electrode. Second, the porous feature of $NiCo_2O_4$ nanosheets increases the amount of electroactive sites and facilitates the electrolyte penetration. Third, the interconnected nanosheets reinforce the electrode structure to withstand the structure collapse upon cycling. Figure 4b reveals SEM image of the $NiCo_2O_4$ nanosheet arrays supported on CF after 3000 cycles. As the figure shows, the structure of the nanosheets is rarely changed without collapse.

In order to investigate the pseudocapacitive performance of the $NiCo_2O_4$/CF electrode, cyclic voltammetry (CV) measurements were performed in a three-electrode cell. Figure 5a displays representative CV profiles of the $NiCo_2O_4$ nanosheet arrays supported on CF within the potential range −0.1−0.5 V (vs SCE)at different scan rates from 5 to 80 mV s^{-1}. Obviously, a pair of peaks is visible in each voltammogram, indicating that the measured capacitance is mainly based on the redox mechanism.[15] Also, the shape of the CV curves is not obviously changed by increasing the scan rate, and the peak current rises with the scan rate, suggesting that the structure of $NiCo_2O_4$/CF composites is beneficial to fast redox reactions. Furthermore, it is evident that the redox peaks shift to lower and higher voltages in higher scan rates, respectively. It may be that the charge transfer kinetics is the limiting step of the reaction.[31,32] The specific capacitances (SC) of the $NiCo_2O_4$/CF electrodes were estimated from CV profiles according to eq 1. The specific capacitance of $NiCo_2O_4$ nanosheet arrays on CF was calculated to be 2172 F g^{-1} at a scan rate of 5 mV s^{-1} and even 743 F g^{-1} at 80 mV s^{-1}.

The properties of the electrode for supercapacitors were studied with chronopotentiometry tests between −0.1 and 0.35 V (vs SCE) at different current densities. Figure 5b shows the charge/discharge curves at current densities ranging from 2 to 20 A g^{-1}. Considering CF only contributes very small capacitance (Figure 6a), the SC of CF was neglected. We calculate the specific capacitance in this method based on eq 2. The SCs are 2658, 2200, 2170, 2000, 1866 F g^{-1} at different current densities of 2, 5, 10, 15, and 20 A g^{-1}, respectively (Figure 5c). This result reveals about 70% of the initial SC remaining even at a high current density of 20 A g^{-1}, indicating that our as-obtained $NiCo_2O_4$/CF composites have excellent rate performance than the reported results.[15,19,29] This might be attributed to high surface area of the ultrathin porous nanosheets electrode structure, which can provide massive electroactive sites and facilitate transport of the electrolyte. More importantly, each interconnected nanosheet can directly contact with CF substrate, which is of good electrical conductivity and shortens the diffusion paths of the electron. The cycling performance of the $NiCo_2O_4$ nanosheet arrays supported on CF were carried out at a current density of 10 A g^{-1}, and the results are shown in Figure 5d. As the figure shows, the SC of the electrode reduced approximately 20% after 3000 cycles. The structure of the $NiCo_2O_4$/CF composites is rarely changed after 3000 cycles (Figure 4b). Thus, the $NiCo_2O_4$/CF

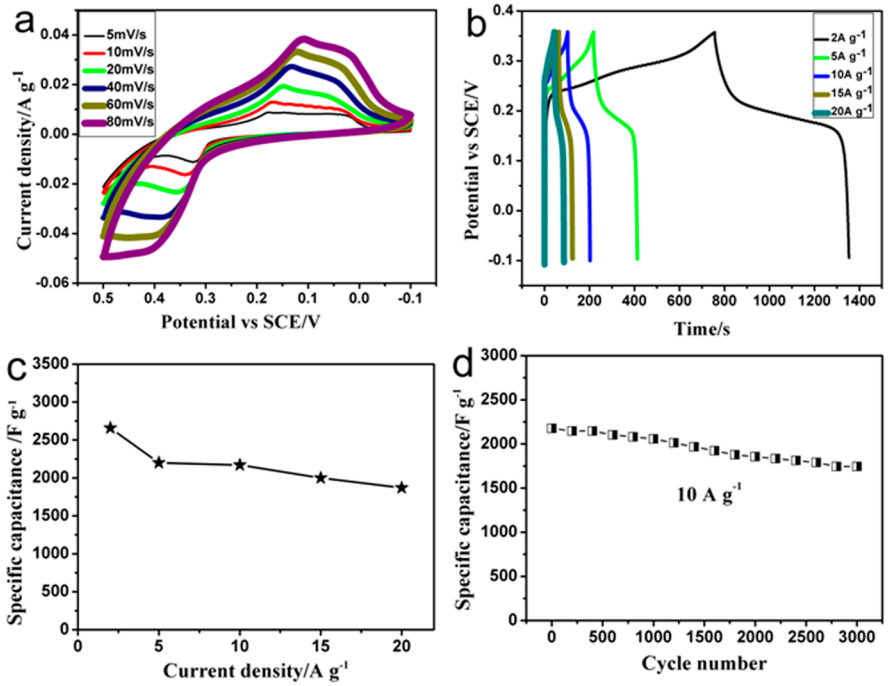

Figure 5. Electrochemical evaluations of the $NiCo_2O_4$/CF composites: (a) CV curves, (b) galvanostatic charge−discharge voltage profiles, (c) corresponding SCs at different current densities, (d) cycling performance at a current density of 10 A g^{-1}.

dx.doi.org/10.1021/am4017335 | ACS Appl. Mater. Interfaces 2013, 5, 7405−7409

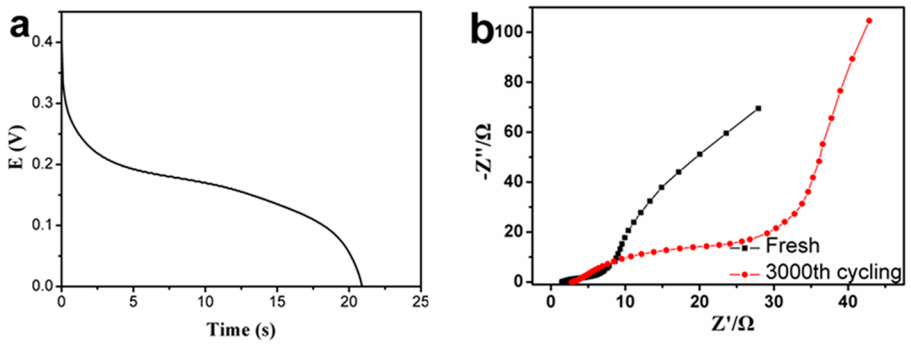

Figure 6. (a) Discharge voltage profile of CF at a current density of 1 A g^{-1}. (b) Nyquist curve of the $NiCo_2O_4$/CF composites before and after 3000 cycling.

composites electrode shows high electrochemical stability for long cycle life.

Impedance spectra of the $NiCo_2O_4$ nanosheet arrays supported on CF were measured to further know the change of as-obtained $NiCo_2O_4$ materials after 3000 cycles. Figure 6b shows the Nyquist profiles of the $NiCo_2O_4$/CF composites before and after 3000 cycles. The impedance spectra include a sloped line in the low-frequency and one semicircle in the high-frequency. We can draw two conclusions from the two spectra. First, in the high frequency area, the solution resistance (R_s) after 3000 cycles increased from 1.5 Ω to 2.8 Ω at the high-frequency intercept of the real axis, indicating the electron conductivity of $NiCo_2O_4$/CF electrode represents a decline tendency. In addition, the diffusive resistance (Warburg impedance) of $NiCo_2O_4$ electrode was a little higher after 3000 cycles in lower frequencies. These results may be because the surface and microstructural changes of the $NiCo_2O_4$ nanoparticles after 3000 successive cycles.

4. CONCLUSIONS

In conclusion, we have prepared an ultrathin $NiCo_2O_4$ nanosheet arrays on flexible CF with strong adhesion for high-performance supercapacitors. The preparation process involves a coelectrodeposition of bimetallic (Ni, Co) hydroxide precursor on CF, and subsequent thermal conversion into $NiCo_2O_4$. The $NiCo_2O_4$/CF composites delivered a high specific capacitance of 2658 F g^{-1} at 2 A g^{-1} (even 1866 F g^{-1} at 20 A g^{-1}) and long cycling life. The as-obtained $NiCo_2O_4$/CF composites are expected to be potentially applied for flexible supercapacitors or other electrochemical devices.

AUTHOR INFORMATION

Corresponding Author

*Tel: +86 731 88822332. Fax: +86 731 88822332. E-mail: lbchen@hnu.edu.cn.

Notes

The authors declare no competing financial interest.

ACKNOWLEDGMENTS

This work was supported by the National Natural Science Foundation of China (Grant Nos. 21103046 and 21003041).

REFERENCES

(1) Simon, P.; Gogotsi, Y. *Nat. Mater.* **2008**, *7*, 845−854.
(2) Yuan, C. Z.; Gao, B.; Shen, L. F; Yang, S. D.; Hao, L.; Lu, X. J.; Zhang, F.; Zhang, L. J.; Zhang, X. G. *Nanoscale* **2011**, *3*, 529−545.
(3) Liu, C.; Li, F.; Ma, L. P.; Cheng, H. M. *Adv. Mater.* **2010**, *22*, E28−E62.
(4) Lei, Z. B.; Christov, N.; Zhao, X. S. *Energy Environ. Sci.* **2011**, *4*, 1866−1872.
(5) Chen, Z.; Qin, Y. C.; Weng, D.; Xiao, Q. F.; Peng, Y. T.; Wang, X. L.; Li, H. X.; Wei, F.; Lu, Y. F. *Adv. Funct. Mater.* **2009**, *19*, 3420−3426.
(6) Yuan, C. Z.; Chen, L.; Gao, B.; Su, L. H.; Zhang, X. G. *J. Mater. Chem.* **2009**, *19*, 246−252.
(7) Sugimoto, W.; Iwata, H.; Yasunaga, Y.; Murakami, Y.; Takasu, Y. *Angew. Chem., Int. Ed.* **2003**, *42*, 4092−4096.
(8) Lu, X. H.; Zheng, D. Z.; Zhai, T.; Liu, Z. Q.; Huang, Y. Y.; Xie, S. L.; Tong, Y. X. *Energy Environ. Sci.* **2011**, *4*, 2915−2921.
(9) Roberts, A. J.; Slade, R. C. T. *J. Mater. Chem.* **2010**, *20*, 3221−3226.
(10) Xu, C. L.; Zhao, Y. Q.; Yang, G. W.; Li, F. S.; Li, H. L. *Chem. Commun.* **2009**, *48*, 7575−7577.
(11) Xia, X. H.; Tu, J. P.; Mai, Y. J.; Wang, X. L.; Gu, C. D.; Zhao, X. B. *J. Mater. Chem.* **2011**, *21*, 9319−9325.
(12) Lee, J. W.; Ahn, T.; Kim, J. H.; Ko, J. M.; Kim, M. D. *Electrochim. Acta* **2011**, 4849−4857.
(13) Xie, K.; Li, J.; Lai, Y. Q.; Lu, W.; Zhang, Z.; Liu, Y. X.; Zhou, L.; Huang, H. T. *Electrochem. Commun.* **2011**, *13*, 657−660.
(14) Xiao, J. W.; Yang, S. H. *RSC Adv.* **2011**, *1*, 588−595.
(15) Wang, H. L.; Gao, Q. M.; Jiang, L. *Small* **2011**, *7*, 2454−2459.
(16) Wei, T. Y.; Chen, C. H.; Chien, H. C.; Lu, S. Y.; Hu, C. C. *Adv. Mater.* **2010**, *22*, 347−351.
(17) Wang, H. X.; Hu, Z. A.; Chang, Y. Q.; Chen, Y. L.; Wu, H. Y.; Zhang, Z. Y.; Yang, Y. Y. *J. Mater. Chem.* **2011**, *21*, 10504−10511.
(18) Tavares, A. C.; Cartaxo, M. A. M.; Pereira, M. I.; da, S.; Costa, F. M. *J. Solid State Electrochem.* **2001**, *5*, 57−67.
(19) Jiang, H.; Man, J.; Li, C. Z. *Chem. Commun.* **2012**, *48*, 4465−4467.
(20) Liu, J. P.; Li, Y. Y.; Huang, X. T.; Li, G. Y.; Li, Z. K. *Adv. Funct. Mater.* **2008**, *18*, 1448−1458.
(21) Jiang, H.; Ma, J.; Li, C. Z. *Chem. Commun.* **2012**, *48*, 4465−4467.
(22) Kaempgen, M.; Chan, C. K.; Ma, J.; Cui, Y.; Gruner, G. *Nano Lett.* **2009**, *5*, 1872−1876.
(23) Hu, L. B.; Choi, J. W.; Yang, Y.; Jeong, S.; Mantia, F. L.; Cui, L. F.; Cui, Y. *Proc. Natl. Acad. Sci. U.S.A.* **2009**, *106*, 21490−21494.
(24) Pushparaj, V. L.; Shaijumon, M. M.; Murugesan, A. K. S.; Ci, L.; Vajtai, R.; Linhardt, R. J.; Nalamasu, O.; Ajayan, P. M. *Proc. Natl. Acad. Sci. U.S.A.* **2007**, *104*, 13574−13577.
(25) Hu, L. B.; Pasta, M.; Mantia, Fabio, L.; Cui, L. F.; Jeong, S.; Deshazer, H. D.; Choi, J. W.; Han, S. M.; Cui, Y. *Nano Lett.* **2010**, *10*, 708−714.
(26) Jiang, H.; Zhao, T.; Ma, J.; Yan, C. Y.; Li, C. Z. *Chem. Commun.* **2011**, *47*, 1264−1266.
(27) Reddy, A. L. M.; Shaijumon, M. M.; Gowda, S. R.; Ajayan, P. M. *Nano Lett.* **2009**, *9*, 1002−1006.

(28) Wu, J. B.; Lin, Y. X.; Xia, H.; Xu, J. Y.; Shi, Q. Y. *Electrochim. Acta* **2011**, *56*, 7163−7170.
(29) Yuan, C. Z.; Li, J. Y.; Hou, L. R.; Zhang, X. G.; Shen, L. F.; Lou, X. W. *Adv. Funct. Mater.* **2012**, *22*, 4592−4597.
(30) Zhang, G. Q.; Wu, H. B.; Hoster, H. E.; Park, M. B. C.; Lou, X. W. *Energy Environ. Sci.* **2012**, *5*, 9453−9456.
(31) Chen, S.; Zhu, J. W.; Wu, X. D.; Han, Q. F.; Wang, X. *ACS Nano* **2010**, *4*, 2822−2830.
(32) Wei, W. F.; Cui, X. W.; Chen, W. X.; Ivey, D. G. *J. Power Sources* **2009**, *186*, 543−550.